Quantification Calibration

For quantification calibration, radioactivity of ^{213}Bi was determined on the gamma-spectrum count rate measured with a high-purity germanium detector (Canberra Industries Inc.). The counting efficiency of the HPGe detector at 440 keV was determined using a known amount of ^{225}Ac activity provided and calibrated at the ITU with a high-resolution gamma spectrometer (*1,2*). The measurements showed an accuracy of 10%.

For converting reconstructed images in Nifti index (Nii) values to MBq, a calibration factor (in MBq/nii) was determined (*3*). To this end, a point source of 70 MBq ^{213}Bi (volume 0.6 mL) in an Eppendorf tube was placed in the center of VECTor and scanned in 30 minutes net measuring time.

Calibration factors to convert the image NII values into MBq are indicated in Table 2.

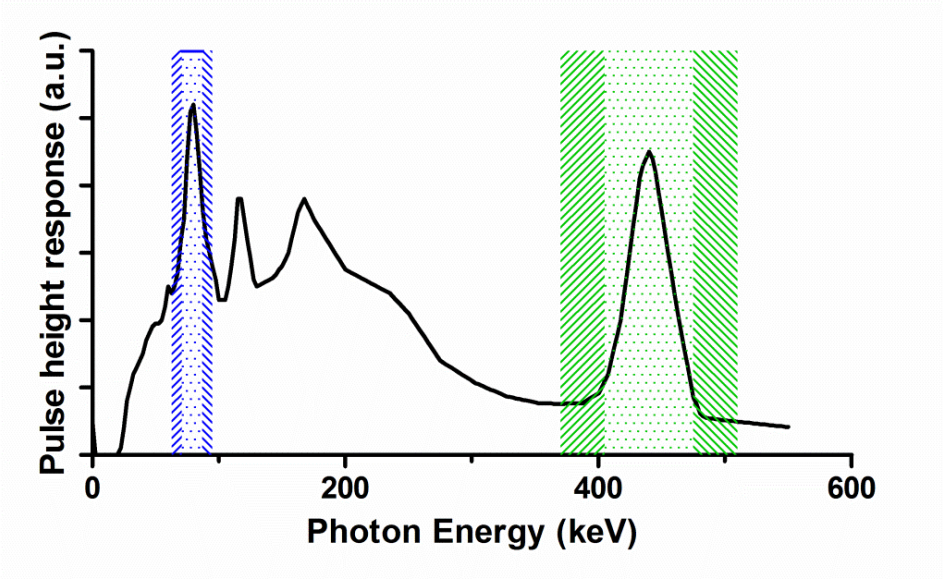

Supplemental Figure 1. Measured pulse height distribution of ^{213}Bi. The 440 keV photopeak window setting (width 16%: 405-475 keV) is represented by the green dotted area. The adjacent green striped areas represent the background windows (width 35 keV: 307-405 and 475-510 keV) used for scatter correction. The dotted blue area represent the 79 keV window (width: 20%: 71-87 keV) and the striped blue areas are the background windows (width 8 keV: 63-71 and 87-95 keV).

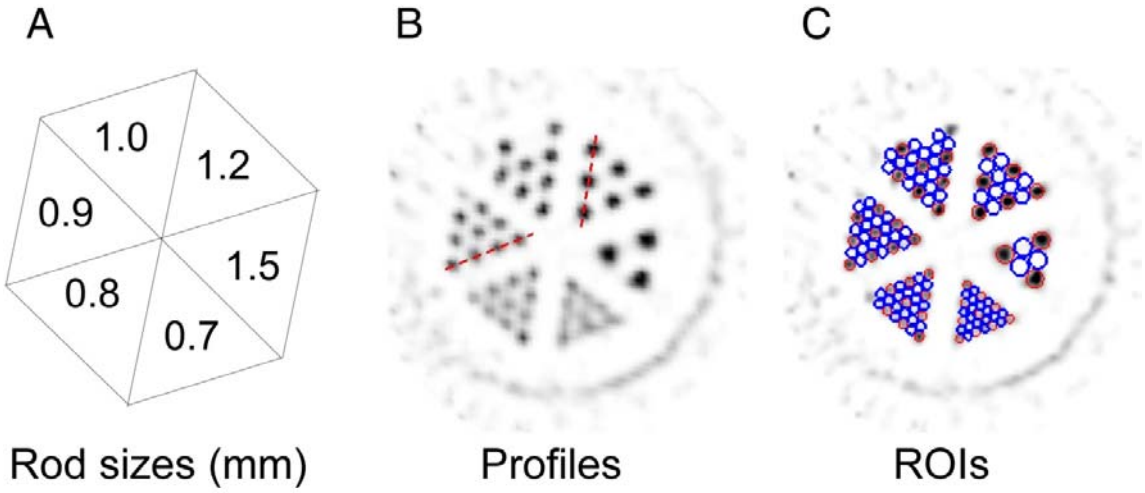

Supplemental Figure 2. Resolution phantom images of ^{213}Bi SPECT. A. Phantom has 6 segments containing capillary diameters of 1.5, 1.2, 1.0, 0.9, 0.8 and 0.7 mm. B. Across 0.9 and 1.2 mm diameter rods profiles were drawn. C. Position of the ROI's to obtain contrast and contrast-to-noise ratios.

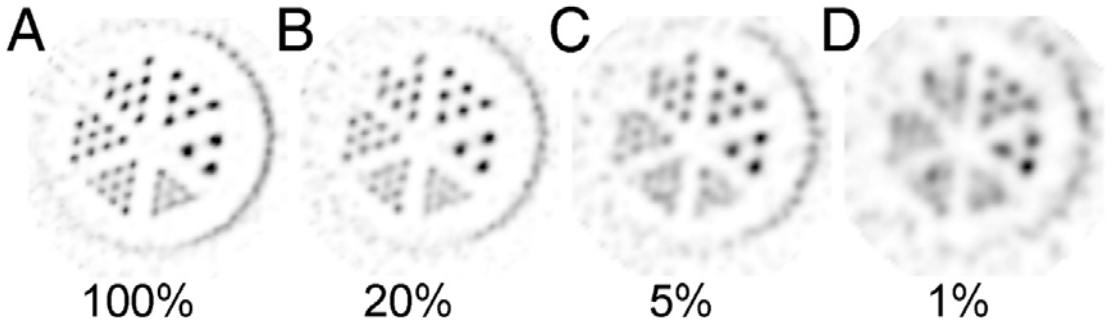

Supplemental Figure 3. Resolution phantom images for the same phantom as shown in figure 3 for various count levels. Reconstructions were based on (A) all listmode data or (B) 20%, (C) 5%, (D) 1% of all detected counts. The combined 79 keV/ 440 keV photopeak window setting was used. Post-reconstruction 3D Gaussian filters with 0.4, 0.6, 0.9, and 1.0 mm FWHM were applied to (A-D).

Supplemental Table 1. Radiation characteristics of ^{213}Bi and its decay-chain daughters. In this table the half-lives of the listed isotopes are shown, as well as the transition energy E for the emission of the listed particles, and the emission yield per transition Y_i. (*4, 5, 6*).

	Yield	Decay	α particles		β particles		γ-rays		X-rays	
	ratio	$T_{1/2}$	E (MeV)	Y_i (/nt)	$\bar{E}$ (keV)	Y_i (/nt)	E (keV)	Y_i (/nt)	E (keV)	Y_i (/nt)
^{213}Bi		45.62 min	5.878	0.0214	435	0.9786	440.5	0.261	77.1	0.0121
									79.6	0.0202
^{213}Po	0.9786	3.708 μs	8.375	1.0						
^{209}Tl	0.0214	2.16 min			656	1.0	117.2	0.843	73.0	0.0635
							465.1	0.969	75.3	0.107
							1567	0.998	85	0.035
^{209}Pb		3.232 h			198	1.0				

Supplemental Table 2. Calibration Factors (CF) using energy windows around the 79 keV X-ray peak, the 440 keV gamma ray peak, or the 79 keV and 440 keV peaks combined.

Energy window	**79 keV**		**440 keV**		**79 keV + 440 keV**	
Voxel size	**0.8 mm**	**0.4 mm**	**0.8 mm**	**0.4 mm**	**0.8 mm**	**0.4 mm**
CF (MBq/Nii)	**16560**	**16440**	**2260**	**2220**	**1850**	**1820**

References

1. Ma D, McDevitt MR, Finn RD, Scheinberg DA. Breakthrough of 225Ac and its radionuclide daughters from an 225Ac/213Bi generator: development of new methods, quantitative characterization, and implications for clinical use. *Appl Radiat Isot.* 2001;55:667-678.

2. McDevitt MR, Finn RD, Sgouros G, Ma D, Scheinberg DA. An 225Ac/213Bi generator system for therapeutic clinical applications: construction and operation. *Appl Radiat Isot.* 1999;50:895-904.

3. Wu C, van der Have F, Vastenhouw B, Dierckx RA, Paans AM, Beekman FJ. Absolute quantitative total-body small-animal SPECT with focusing pinholes. *Eur J Nucl Med Mol Imaging.* 2010;37:2127-2135.

4. Jaggi JS, Seshan SV, McDevitt MR, LaPerle K, Sgouros G, Scheinberg DA. Renal tubulointerstitial changes after internal irradiation with alpha-particle-emitting actinium daughters. *J Am Soc Nephrol.* 2005;16:2677-2689.

5. Vaissier PE, Goorden MC, Vastenhouw B, van der Have F, Ramakers RM, Beekman FJ. Fast spiral SPECT with stationary gamma-cameras and focusing pinholes. *J Nucl Med.* 2012;53:1292-1299.

6. Vastenhouw B, Beekman F. Submillimeter total-body murine imaging with U-SPECT-I. *J Nucl Med.* 2007;48:487-493.